AUT Journal of Electrical Engineering
10.22060/EEJ.2024.23555.5623

Presenting an Automatic Hierarchical Method to Segmentation of Pulmonary Nodules in CT-Scan Images

Marzia Asadi[1], Hamid Hassanpour[2]

[1]MSc, Faculty of Computer Engineering and IT, Shahrood University of Technology, Shahrood, Iran
[2]PhD, Faculty of Computer Engineering and IT, Shahrood University of Technology, Shahrood, Iran

*Corresponding author: h.hassanpour@shahroodut.ac.ir

Abstract:

Pulmonary nodules are significant factors in the development of lung cancer, making timely identification crucial for effective patient management. This study introduces a fully automated method employing a two-stage deep learning approach for the segmentation of pulmonary nodules in CT scan images. In the first stage, we utilize a deep learning network known as BCD-Unet to extract the lung region from the CT scans. The second stage employs another deep learning network that incorporates attention mechanisms and residual modules for the precise segmentation and extraction of pulmonary nodules within the identified lung region. The proposed algorithm was rigorously tested on the LUNA16 dataset, yielding impressive results: a Dice coefficient of 97.75 for lung segmentation, alongside a Dice coefficient of 91.73% and a sensitivity of 92.31% for nodule segmentation. These findings underscore the effectiveness of the proposed method in enhancing the accuracy of pulmonary nodule detection, which is vital for early intervention in lung cancer cases. Also, this research contributes significantly to the field of medical imaging and has important implications for clinical practice in lung cancer management.

Keywords:

Attention-Unet; BCD-Unet; Histogram Equalization; Image Segmentation; Lung Nodules

10.22060/EEJ.2024.23555.5623

1. Introduction

Lung cancer continues to be one of the leading causes of cancer-related mortality globally[1,2], highlighting the urgent need for early detection and diagnosis. Identifying and segmenting pulmonary nodules, which may indicate lung malignancies, is a complex task due to various challenges associated with nodule characteristics and imaging conditions. These challenges include variability in nodule size, shape, and density, as well as the presence of artifacts and noise in CT scans, which can hinder accurate detection and segmentation.

Over the years, various approaches have been developed for pulmonary nodule detection, primarily categorized into combined feature engineering and image processing methods and deep learning techniques[3-5]. Classical image processing methods while often straightforward and interpretable, face limitations in handling complex nodule presentations and may require extensive manual tuning of parameters. In contrast, deep learning approaches[6] have shown significant promise in enhancing performance metrics such as sensitivity and specificity, as they can automatically learn features from data. However, these methods also encounter challenges, including the need for large annotated datasets and the risk of overfitting in cases of limited data diversity.

Given the critical importance of detecting and diagnosing lung diseases, significant efforts have been dedicated over the years to enhancing various interrelated research areas, including lung segmentation [7-10], lung nodule segmentation and detection [3-5], and the diagnosis of other pulmonary conditions [11,12]. Lung nodule segmentation, the primary focus of this study, has seen considerable advancements that can be categorized into classical image processing techniques [13] and deep learning approaches.

Classical methods focused on strategies such as morphological operators [14,15], region growing [16,17], edge detection-based methods [18,19], and some synthesized image processing-based algorithms combined with classic learning methods [20-22].

Ugar and Selin [14] used basic algorithms of image processing, including erosion operations, median noise reduction filters, and Otsu thresholding, for the extraction of lung nodules from CT images. In this activity, an erosion operation is first used to smooth the image and remove small sections within

the lung area. The next step involved using a median filter to eliminate noise. Subsequently, the algorithm utilizes Otsu thresholding to separate different regions of the image and the lung. To remove small image noises resulting from the Otsu operation, a morphological operation is applied. Finally, by subtracting the two images obtained from Otsu thresholding and removing the regions identified during the morphological operation, the location of the nodule in the image is determined.

In Kalaria et al. [16], the Sobel edge detection method combined with morphological algorithms was used to identify the lungs and pulmonary nodules. In their work, the Sobel algorithm was initially employed to extract the lungs from the image. In the next step, noise was cleared through a morphological process and the binary image was cleaned in relation to the desired mask. Finally, the nodules were identified using the definition of connected components. Among classical image processing methods, the region-growing method has been widely utilized compared to others.

Savic et al. [18] used an improved region-growing algorithm for the identification of pulmonary nodules. They applied a Fast-Marching algorithm to segment the image into regions with similar characteristics. Then, for the regions obtained, they combined the results of the Fast-Marching algorithm with the region-growing method and k-means clustering.

Segmentation methods based on classical image processing algorithms combined with some classical machine learning methods are usually with clear structural processes, fast, and have low computational complexity. However, they require manual tuning for parameters. In contrast to classic image processing methods, there are deep learning algorithms where the main idea is to use deep convolutional networks, typically based on U-Net structures [23]. For instance, one can refer to the work of Xiapu et al. [24], who used an improved V-Net model for nodule segmentation. In their model, they implemented a residual module and an attention mechanism to enhance feature extraction and reduce the false positive rate. Although the method presented in this research has good accuracy, the computational complexity of the proposed model is high.

In another study, Zhang et al. [25] used a multiscale feature extraction model for the segmentation of lung nodules. They applied two combined modules, called the improved residual module and the dense module, for better feature extraction. An important point in Zhang et al.'s research was the high complexity of the algorithm due to the use of multiple dense modules, which reduced the processing

10.22060/EEJ.2024.23555.5623

speed of the learning model. Generally, deep learning methods, despite having high accuracy and being fully automatic, exhibit high computational complexity. Another point in the segmentation of nodules in various studies is that the segmentation operation is usually performed on a section of images in which pulmonary nodules are present. In the next section, the proposed method will be explained.

In our work, we propose a novel three-stage methodology for effective pulmonary nodule segmentation. This approach begins with a preprocessing step to enhance the quality of CT images, followed by a two-step deep learning framework comprising consecutive deep neural networks to accurately identify both lung regions and pulmonary nodules. This systematic methodology aims to overcome existing challenges and improve the accuracy of nodule detection.

In this paper, Section 2 present our proposed methodology. The results of our experiments are presented in Section 3, demonstrating the efficacy of our approach. Finally, Section 4 concludes with a summary of our findings and their implications for future research in lung cancer detection and management.

2. Theoretical and Experimental Modeling

In this section, we will describe the proposed method, as illustrated in Fig. 1. Below, the details of each step in the proposed method are described

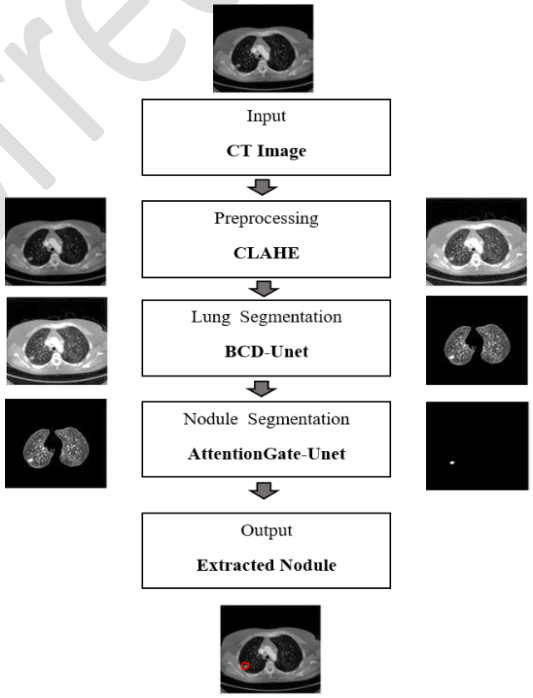

Fig. 1. Diagram of proposed method for nodule segmentation

10.22060/EEJ.2024.23555.5623

2-1- Preprocessing

In this study, we employ Contrast Limited Adaptive Histogram Equalization (CLAHE) [26] as a preprocessing technique to enhance the quality of CT images prior to segmentation. CLAHE is particularly effective in improving the contrast of images while preventing the over-amplification of noise, which is crucial for medical imaging applications. CLAHE operates by dividing the image into small, non-overlapping regions known as tiles. For each tile, it computes the histogram and applies histogram equalization to enhance contrast. However, to avoid noise amplification in homogeneous areas, CLAHE introduces a limit on the contrast enhancement. The steps involved in CLAHE can be summarized as follows:

Step 1. Tile Division: The input image $I(x, y)$ is divided into N tiles of size $M \times M$.

Step 2. Histogram Computation: For each tile T_i, the histogram H_i is computed.

Step 3. Contrast Limiting: A predefined clip limit C is applied to the histogram to limit the maximum height of the histogram bins. This prevents excessive contrast enhancement:

$$H_i^{'} = \begin{cases} H_i & ; H_i \le C \\ C & ; H_i > C \end{cases} \quad (1)$$

In Eq. (1), H_i is the maximum frequency(height) histogram of tile T_i. if H_i is less than C, the height of between the histograms in tile T_i does not change. This means that in this tile the contrast is proper and don't needs to modification. But if H_i is greater than of C, maximum frequency of histogram of tile T_i must limit. So, H_i modified to H'_i. This avoids over-enhancing the contrast in homogeneous areas that may contain noise.

Step 4. CDF Calculation: The cumulative distribution function (CDF) for each clipped histogram is calculated and normalized.

Step 5. Pixel Value Mapping: Each pixel in the tile is mapped to a new intensity value based on the normalized CDF as seen in Eq. (2):

$$I_{inhanced}\left(x, y\right) = CDF_i\left(I\left(x, y\right)\right) \quad (2)$$

Step 6. Interpolation: To ensure smooth transitions between adjacent tiles, bilinear interpolation is applied at the borders of the tiles.

10.22060/EEJ.2024.23555.5623

By applying CLAHE, we obtain an enhanced image $I_{inhanced}(x, y)$, which exhibits improved contrast and better visibility of pulmonary nodules. This enhancement is crucial for subsequent segmentation tasks, allowing deep learning models to effectively identify and delineate nodules within lung regions. Fig. 2 shown the effect of CLAHE for a CT image.

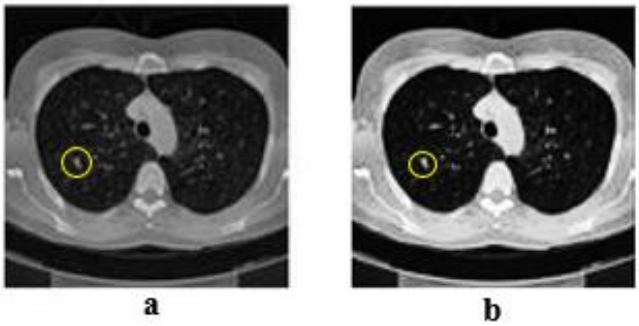

a) original image, b) CLAHE improvement
Fig. 2. Effect of Histogram equalization by CLAHE

2-2- Lung Segmentation

For lung segmentation, we use a Bi-directional ConvLSTM U-Net with Densely Connected Convolutions (BCD-Unet) deep neural network introduced by Azad et al. [10]. BCD-Unet is a model based on U-Net that is used for various applications in medical image processing [10], especially for image segmentation. This model leverages the bidirectional ConvLSTM module [27] to enhance its performance. The following describes this module.

A) BConvLSTM Module

ConvLSTM is a specialized type of recurrent neural network used for spatio-temporal forecasting, characterized by its convolutional structures in both transitions from input to state and from state to state. This model forecasts the future state of a specific cell in a grid based on the inputs and the previous states of its neighboring cells. This is accomplished by applying a convolution operator during the transitions from state to state and from input to state (refer to Figure 3). The mathematics of this module are explained in [27]. Fig. 3 demonstrate ConvLSTM module. The ConvLSTM processes sequential data by maintaining a hidden state across time steps. In this architecture h_{t-1}represents the hidden tensor from the previous layer, which carries information from the prior time step. The current hidden tensor h_t is

computed based on the input x_t at the current time step and the previous hidden state h_{t-1}. Finally, h_{t+1} serves as the output hidden tensor for the next time step, encapsulating the information necessary for future predictions. Additionally, x_{t+1} indicates the output of the current time step, which will be utilized as the input for the next step.

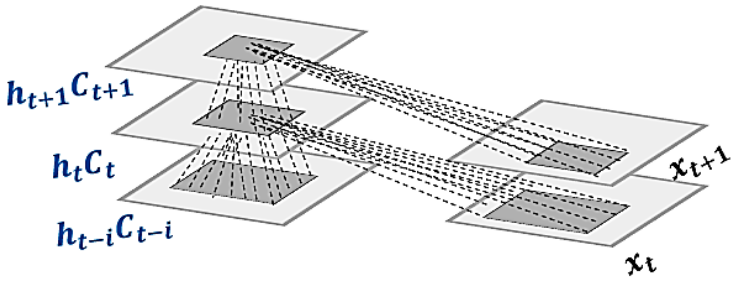

Fig. 3. Structure of ConvLSTM [27]

- **Input-to-state and state-to-state transitions:** Convolution operations are used instead of traditional matrix multiplication.
- **Memory Cell:** Similar to LSTM, it includes input, output, and forget gates, but these operations are applied spatially.

B) BCD-Unet Architecture

BCD-Unet uses ConvLSTM layers as part of its architecture to better model spatio-temporal information for segmenting the lung region. The architecture of BCD-Unet is indicated in Figure 4. As seen in Fig. 4, the ConvLSTM module is placed in the middle part of the network and in the skip connection part between each encoder block and its corresponding decoder block.

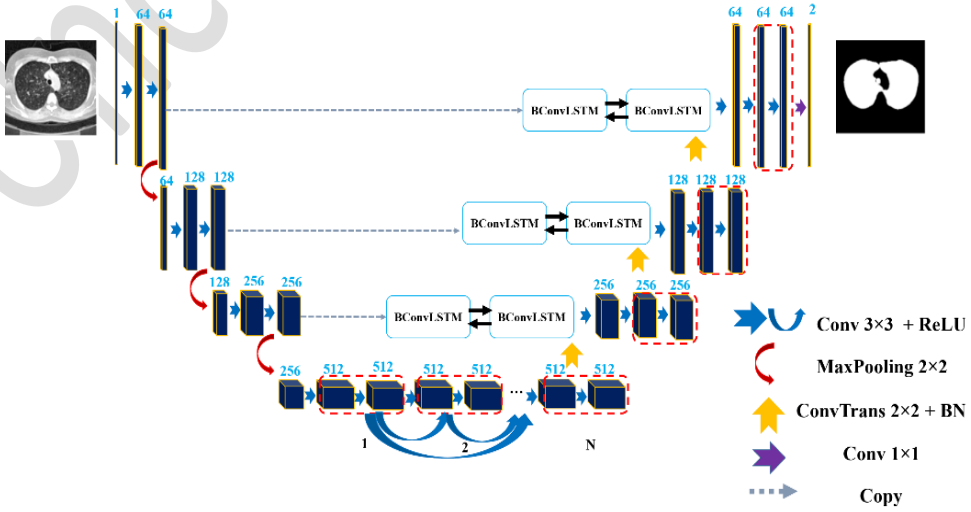

Fig. 4. BCD-Unet Architecture.

10.22060/EEJ.2024.23555.5623

2-3-Nodule Segmentation

By Considering the size of pulmonary nodules in CT images are small, feature extraction should be done in different dimension using convolution layers. For this purpose, using the attention mechanism can be efficient. In the following, the details of the attention mechanism will be explained.

Attention Mechanism: The attention mechanism [28] is a computational strategy that enables models to concentrate on specific parts of the input data while disregarding others. This concept has been widely used in computer vision due to its effectiveness in enhancing model performance and interpretability. In this context, attention mechanisms help models prioritize certain regions of an image when making predictions or generating features. This approach mimics human visual perception, where we tend to focus on areas of interest while processing visual information. Fig. 5 illustrates the concept of attention. As shown, by focusing on the image, regions that are more significant and likely to contain nodules are assigned higher weights for segmentation. In fact, by using this mechanism, we can explore the details which allows models to focus on the most relevant parts of the input data while disregarding irrelevant information

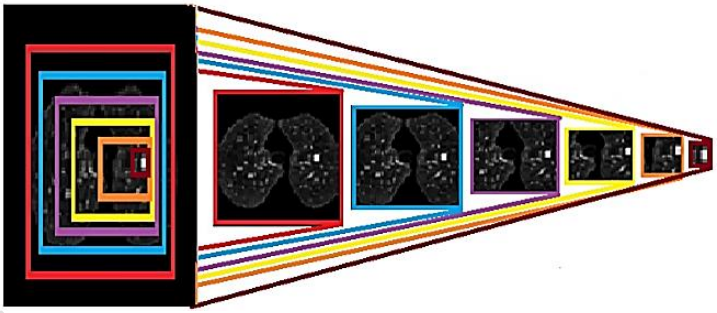

Fig. 5. Focusing on important points in the image as concept of attention mechanism

In fact, by employing Attention U-Net for nodule segmentation, the network extracts features across different dimensions, directing its focus toward the areas with greater weight to identify the nodule. Fig. 6 demonstrates the architecture of the Attention U-Net used in this research.

10.22060/EEJ.2024.23555.5623

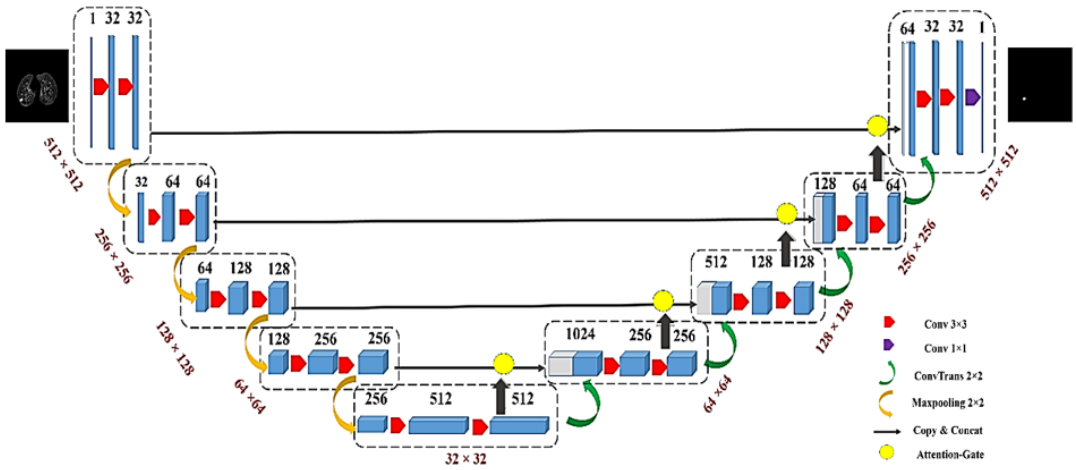

Fig. 6. Attention-Unet Architecture for nodule segmentation

2-4- Summary of Proposed Method

In the proposed method for steps A to C, Table1 summarizes the implementation details for BCD-Unet and Attention U-Net.

Table1. Features of implemented Networks

Features	BCD-Unet	Attention-Unet
Parameters	20659717	8114017
Epoch	50	150
Loss	Binary Cross Entropy	Binary Cross Entropy
Optimizer	Adam	Adam
Learning-Rare	0.001	0.001
Metric	Dice , Sensitivity	Dice , Sensitivity

Novelties of the Proposed Method

In this study, we introduce a novel three-stage methodology that combines the strengths of two advanced deep learning architectures, BCD-Unet and Attention U-Net, to address the complex task of pulmonary nodule segmentation. While individual architectures have been effectively utilized in prior works, our approach is unique in several key aspects:

- **Complementary Segmentation Enhancements:** By employing BCD-Unet for lung region segmentation and subsequently utilizing Attention U-Net for nodule segmentation, we are able to

leverage the spatial and contextual information more effectively. This two-stage approach enhances the precision of nodule detection, particularly in regions where nodules are small and may be easily overlooked.

- **Attention Mechanism Integration:** The incorporation of an attention mechanism within the U-Net framework allows the model to focus on significant areas of the lung that are likely to contain nodules. This focus on relevant regions is not only beneficial for improving segmentation accuracy but also aids in reducing false positives, which is crucial for clinical applications.
- **Enhanced Preprocessing Techniques:** The use of Contrast Limited Adaptive Histogram Equalization (CLAHE) as a preprocessing step is another unique aspect of our method. This technique effectively enhances image contrast while avoiding noise amplification, thereby creating a more favorable input for the subsequent deep learning models. This step is vital for improving model performance, particularly in images with varying densities and noise.

In next section will investigated experimental results.

3. Results

In this section, we aim to examine the results obtained from the proposed algorithm. To this end, we will first introduce the dataset, then explain the Dice and sensitivity metrics, and finally present visual results and comparisons with related works.

In this study, we primarily focused on comparing our proposed deep learning approaches, namely BCD-Unet and Attention U-Net, with other state-of-the-art deep learning methods used for pulmonary nodule segmentation. The rationale behind our decision to limit comparisons to deep learning algorithms is based on several factors:

- **Advancements in Deep Learning**: Recent advancements in deep learning techniques have demonstrated significant improvements in image segmentation tasks, particularly in the domain of medical imaging. While classical image processing methods provide foundational approaches, they often struggle with the complexities and variabilities of medical images, such as lung nodules. By

concentrating on deep learning methodologies, we aimed to showcase the efficacy and robustness of our approach within the context of current state-of-the-art solutions.

- **Focus on Feature Learning:** Deep learning models, such as BCD-Unet and Attention U-Net, inherently perform feature learning from the data, allowing them to adapt and optimize their performance based on large amounts of annotated data. Classical methods, on the other hand, rely heavily on handcrafted features, which may not generalize well across diverse datasets. Consequently, the comparison of our method with other deep learning algorithms provides a more relevant benchmark for assessing the potential enhancements in segmentation accuracy and performance.
- **Context of Clinical Application:** In clinical practice, the trend is increasingly shifting towards the adoption of deep learning methods for automated image analysis. Therefore, highlights of our research are most appropriately contextualized within a comparison to similar advanced algorithms rather than to traditional techniques that may no longer be as widely utilized in contemporary research and applications.

Despite these considerations, we acknowledge the historical relevance and contributions of classical image processing techniques. Future work may include comparative analyses with such methods to explore their relative strengths and weaknesses comprehensively.

3-1- Dataset

In this study, we utilized the LUNA16 dataset [29], which consists of a collection of lung nodule CT scans. The dataset includes 1,186 annotated images specifically designed for the segmentation of lungs and nodules. The images were divided into training and testing sets, with 90% allocated for training and 10% for testing. To prevent overfitting, we utilized the validation split parameter in the fit function during model training, along with the early stopping technique.

3-2- Metrics

Two main criteria were used to compare the proposed method with related research. Additionally, the precision metric is employed to evaluate the percentage of true positives in the segmented target areas

compared to all estimated target regions for detecting and localizing lung nodules in the BCD-Unet and Attention-Unet networks.

A) Sensitivity (True Positive Rate)

Sensitivity[30], also known as the True Positive Rate (TPR), measures the proportion of actual positives that are correctly identified by the model. It is a crucial metric in medical diagnostics, as it reflects the ability of a test to correctly identify patients with a condition. Eq. (3) is mathematical concept of sensitivity.

$$sensitivity = \frac{TP}{TP + FN} \tag{3}$$

In Eq. (3), True Positives (*TP*) are the instances that are correctly identified as positive, while False Negatives (*FN*) are the instances that are actually positive but incorrectly identified as negative.

B) Dice Coefficient

The Dice Coefficient[31], also known as the Dice Similarity Coefficient (DSC), is a statistical measure used to gauge the similarity between two sets. In the context of segmentation tasks, it quantifies the overlap between the predicted segmentation and the ground truth. Eq. (4) is mathematic of DSC measurement.

$$DSC = \frac{TP}{TP + FP + FN} \tag{4}$$

Where False Positives (*FP*) are the instances that are incorrectly identified as positive.

C) Precision

Precision[30] is a performance metric used to evaluate the accuracy of a classification model. It is calculated by dividing the number of true positive predictions by the sum of true positive and false positive predictions, indicating how many of the predicted positive cases were actually positive. Eq. (5) represents the mathematical formula for precision.

10.22060/EEJ.2024.23555.5623

$$Precision = \frac{TP}{TP + FP} \tag{5}$$

3-3-Visual Results

In this part, the visual results obtained from the proposed algorithm for each step of lung and nodule segmentation are examined. As shown in Fig. 7 and Fig. 8, the BCD-Unet and Attention-Unet networks have significantly succeeded in performing the segmentation tasks. As seen in Fig. 7, the BCD-Unet network has effectively estimated the lung region when compared to the reference mask output. Additionally as seen in Fig. 8 illustrates the precise location of the nodule in comparison to the reference mask output.

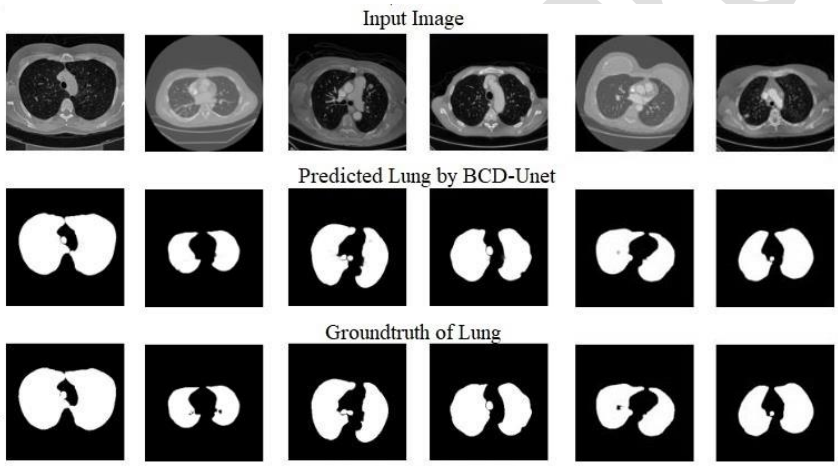

Fig.7 . BCD-Unet lung segmentation Output

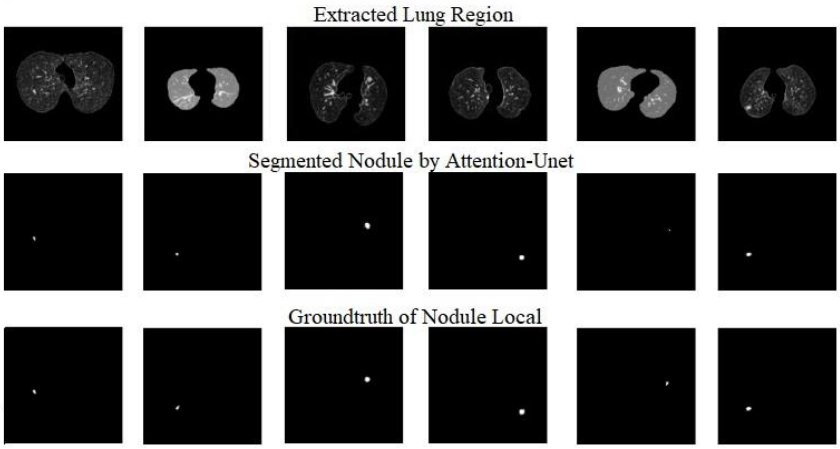

Fig. 8. Attention-Unet nodule segmentation Output

3-4- Comparison

In this part, the results obtained from the proposed method are compared with several related algorithms. we compare result of our proposed method by some other researches on LUNA16 dataset.

Table 2 and Table 3 present the results for the BCD-Unet and Attention-Unet networks based on the Dice and Sensitivity metrics, respectively. As indicated in these tables, both networks performed reasonably well in target recognition.

Table 2: BCD-Unet Lung segmentation

Metric	Train	Test
Sensitivity	98.21	97.81
DSC	97.36	97.75

- **Analysis of Lung Segmentation using BCD-Unet**

The results presented in Table 2 indicate that our proposed BCD-Unet model achieved a Dice coefficient of 97.75 for lung segmentation and a sensitivity of 97.81. Notably, the precision for lung segmentation was found to be 98.73, which demonstrates a high ratio of true positives (*TP*) to false positives (*FP*). This high precision indicates that the model effectively identifies lung regions with minimal misclassification, contributing to its overall performance in accurately segmenting pulmonary structures in CT scans.

Table 3. Attention-Unet Nodule segmentation

Research Architecture	*DSC*	*Sensitivity*
Xitau et al[32] 3D-Res2-Unet	81.22	79.89
Silvan et al[33] Unet GNN	78.84	84.45
Daval et al[34] Advanced Unet	79.22	79.89
Kumar et al[35] Unet	77.84	78.98
Bhattacharyya et al [36] BD-Unet	88.89	90.24
Proposed Method	**91.73**	**92.31**

- **Analysis of Nodule Segmentation using Attention-Unet**

In addition to sensitivity and Dice coefficient, we also calculated the precision for nodule segmentation, which was found to be 90.83. In Table 3, we present a comparison with several existing methods such as Xitau et al. (3D-Res2-Unet) [32], Silvan et al. (Unet GNN)[33], and Bhattacharyya et al. (BD-Unet)[36].

These methods were selected based on their relevance to the pulmonary nodule segmentation task and their reported performance metrics in recent literature.

The chosen methods represent a range of deep learning architectures that have been applied to similar problems in medical imaging. For instance, the 3D-Res2-Unet is known for its ability to capture volumetric data, while the Unet GNN leverages graph neural networks for improved spatial representation. By comparing our proposed method against these contemporaneous approaches, we aim to demonstrate the robustness and efficiency of our model in segmenting pulmonary nodules.

Due to the unavailability of precision metrics for all comparative studies, we focused on presenting Dice coefficients and sensitivity as the two main criteria for a more consistent evaluation. The high precision and other evaluated metrics indicate that our proposed method is not only effective at identifying true positives but also excels in minimizing false positives. This capability is especially important in clinical settings, where accurate identification of pulmonary nodules is essential for timely diagnosis and intervention in lung cancer cases. Overall, these metrics reflect the robustness and reliability of our method, suggesting its significant potential for improving diagnostic accuracy in medical imaging.

4. Conclusion

In this paper, we utilized two networks, BCD-Unet and Attention-Unet, sequentially to identify and segment lung nodules. The BCD-Unet was employed to segment the lung regions, while the Attention-Unet was trained on the output of the BCD-Unet to specifically segment and recognize the nodules. The results demonstrated that the combination of these two networks significantly improved the segmentation of both the lungs and lung nodules in CT images. This approach highlights the effectiveness of using complementary segmentation techniques to enhance diagnostic accuracy in medical imaging. While our study relies solely on the LUNA16 dataset, which may not represent the diversity of lung nodules encountered in clinical practice, this dataset possesses significant importance as a standard for testing. Overall, our findings underline the potential of deep learning models in improving the detection of lung abnormalities, contributing to better patient outcomes. Future research could further explore the integration of multiple datasets to enhance the generalizability of our results.

5. References

[1] R.L. Siegel, A.N. Giaquinto, A. Jemal, Cancer statistics, 2024, CA: a cancer journal for clinicians, 74(1) (2024).
[2] T.B. Kratzer, P. Bandi, N.D. Freedman, R.A. Smith, W.D. Travis, A. Jemal, R.L. Siegel, Lung cancer statistics, 2023, Cancer, 130(8) (2024) 1330-1348.
[3] S. Shamas, S. Panda, I. Sharma, Review on lung nodule segmentation-based lung cancer classification using machine learning approaches, in: Artificial Intelligence on Medical Data: Proceedings of International Symposium, ISCMM 2021, Springer, 2022, pp. 277-286.
[4] A. Halder, D. Dey, A.K. Sadhu, Lung nodule detection from feature engineering to deep learning in thoracic CT images: a comprehensive review, Journal of digital imaging, 33(3) (2020) 655-677.
[5] Y. Gu, J. Chi, J. Liu, L. Yang, B. Zhang, D. Yu, Y. Zhao, X. Lu, A survey of computer-aided diagnosis of lung nodules from CT scans using deep learning, Computers in biology and medicine, 137 (2021) 104806.
[6] R. Aggarwal, V. Sounderajah, G. Martin, D.S. Ting, A. Karthikesalingam, D. King, H. Ashrafian, A. Darzi, Diagnostic accuracy of deep learning in medical imaging: a systematic review and meta-analysis, NPJ digital medicine, 4(1) (2021) 65.
[7] S. Gite, A. Mishra, K. Kotecha, Enhanced lung image segmentation using deep learning, Neural Computing and Applications, 35(31) (2023) 22839-22853.
[8] H.M. Kim, T. Ko, I.Y. Choi, J.-P. Myong, Asbestosis diagnosis algorithm combining the lung segmentation method and deep learning model in computed tomography image, International Journal of Medical Informatics, 158 (2022) 104667.
[9] A. Comelli, C. Coronnello, N. Dahiya, V. Benfante, S. Palmucci, A. Basile, C. Vancheri, G. Russo, A. Yezzi, A. Stefano, Lung segmentation on high-resolution computerized tomography images using deep learning: a preliminary step for radiomics studies, Journal of Imaging, 6(11) (2020) 125.
[10] R. Azad, M. Asadi-Aghbolaghi, M. Fathy, S. Escalera, Bi-directional ConvLSTM U-Net with densley connected convolutions, in: Proceedings of the IEEE/CVF international conference on computer vision workshops, 2019, pp. 0-0
[11] A.T. Abdulahi, R.O. Ogundokun, A.R. Adenike, M.A. Shah, Y.K. Ahmed, PulmoNet: a novel deep learning based pulmonary diseases detection model, BMC Medical Imaging, 24(1) (2024) 51.
[12] S. Kumar, H. Kumar, G. Kumar, S.P. Singh, A. Bijalwan, M. Diwakar, A methodical exploration of imaging modalities from dataset to detection through machine learning paradigms in prominent lung disease diagnosis: a review, BMC Medical Imaging, 24(1) (2024) 30.
[13] P. Kamra, R. Vishraj, S. Gupta, Performance comparison of image segmentation techniques for lung nodule detection in CT images, in: 2015 International Conference on Signal Processing, Computing and Control (ISPCC), IEEE, 2015, pp. 302-306.
[14] S. Uzelaltinbulat, B. Ugur, Lung tumor segmentation algorithm, Procedia computer science, 120 (2017) 140-147.
[15] M.N. Saad, Z. Muda, N.S. Ashaari, H.A. Hamid, Image segmentation for lung region in chest X-ray images using edge detection and morphology, in: 2014 IEEE international conference on control system, computing and engineering (ICCSCE 2014), IEEE, 2014, pp. 46-51.
[16] V. Kalaria, S. Priyadarsini, Morphed Sobel Approach for Detecting Cancer Cells in Lungs, INTERNATIONAL JOURNAL OF ENGINEERING DEVELOPMENT AND RESEARCH, 2(2) (2014) 1751-1758-1751-1758.
[17] L. Ramos, I. Pineda, A Semiautomatic Image Processing-Based Method for Binary Segmentation of Lungs in Computed Tomography Images, SN Computer Science, 5(6) (2024) 689.
[18] M. Savic, Y. Ma, G. Ramponi, W. Du, Y. Peng, Lung nodule segmentation with a region-based fast marching method, Sensors, 21(5) (2021) 1908.
[19] V. Thamilarasi, R. Roselin, Lung segmentation in chest X-ray images using Canny with morphology and thresholding techniques, International Journal of Advance and Innovative Research, 6(1) (2019) 1-7.
[20] C. Liu, R. Zhao, M. Pang, Lung segmentation based on random forest and multi-scale edge detection, IET Image Processing, 13(10) (2019) 1745-1754.

[21] S.Y. Chong, M.K. Tan, K.B. Yeo, M.Y. Ibrahim, X. Hao, K.T.K. Teo, Segmenting nodules of lung tomography image with level set algorithm and neural network, in: 2019 IEEE 7th Conference on Systems, Process and Control (ICSPC), IEEE, 2019, pp. 161-166.
[22] S.M. Naqi, M. Sharif, M. Yasmin, Multistage segmentation model and SVM-ensemble for precise lung nodule detection, International journal of computer assisted radiology and surgery, 13 (2018) 1083-1095.
[23] G. Du, X. Cao, J. Liang, X. Chen, Y. Zhan, Medical Image Segmentation based on U-Net: A Review, Journal of Imaging Science & Technology, 64(2) (2020).
[24] X. Ma, H. Song, X. Jia, Z. Wang, An improved V-Net lung nodule segmentation model based on pixel threshold separation and attention mechanism, Scientific Reports, 14(1) (2024) 4743.
[25] X. Zhang, S. Kong, Y. Han, B. Xie, C. Liu, Lung Nodule CT Image Segmentation Model Based on Multiscale Dense Residual Neural Network, Mathematics, 11(6) (2023) 1363.
[26] P. Musa, F. Al Rafi, M. Lamsani, A Review: Contrast-Limited Adaptive Histogram Equalization (CLAHE) methods to help the application of face recognition, in: 2018 third international conference on informatics and computing (ICIC), IEEE, 2018, pp. 1-6.
[27] X. Shi, Z. Chen, H. Wang, D.-Y. Yeung, W.-K. Wong, W.-c. Woo, Convolutional LSTM network: A machine learning approach for precipitation nowcasting, Advances in neural information processing systems, 28 (2015).
[28] S. Woo, J. Park, J.-Y. Lee, I.S. Kweon, Cbam: Convolutional block attention module, in: Proceedings of the European conference on computer vision (ECCV), 2018, pp. 3-19.
[29] A.A.A. Setio, A. Traverso, T. De Bel, M.S. Berens, C. Van Den Bogaard, P. Cerello, H. Chen, Q. Dou, M.E. Fantacci, B. Geurts, Validation, comparison, and combination of algorithms for automatic detection of pulmonary nodules in computed tomography images: the LUNA16 challenge, Medical image analysis, 42 (2017) 1-13.
[30] G. Naidu, T. Zuva, E.M. Sibanda, A review of evaluation metrics in machine learning algorithms, in: Computer Science Online Conference, Springer International Publishing, Cham, (2023), pp. 15-25.
[31] T. Eelbode, J. Bertels, M. Berman, D. Vandermeulen, F. Maes, R. Bisschops, M.B. Blaschko, Optimization for medical image segmentation: theory and practice when evaluating with dice score or jaccard index, IEEE transactions on medical imaging, 39(11) (2020) 3679-3690.
[32] Z. Xiao, B. Liu, L. Geng, F. Zhang, Y. Liu, Segmentation of lung nodules using improved 3D-UNet neural network, Symmetry, 12(11) (2020) 1787.
[33] A. Garcia-Uceda Juarez, R. Selvan, Z. Saghir, M. de Bruijne, A joint 3D UNet-graph neural network-based method for airway segmentation from chest CTs, in: Machine Learning in Medical Imaging: 10th International Workshop, MLMI 2019, Held in Conjunction with MICCAI 2019, Shenzhen, China, October 13, 2019, Proceedings 10, Springer, 2019, pp. 583-591.
[34] D.D. Kadia, Advanced UNet for 3D Lung Segmentation and Applications, University of Dayton, 2021.
[35] S.N. Kumar, P.M. Bruntha, S.I. Daniel, J.A. Kirubakar, R.E. Kiruba, S. Sam, S.I.A. Pandian, Lung nodule segmentation using unet, in: 2021 7th International conference on advanced computing and communication systems (ICACCS), IEEE, 2021, pp. 420-424.
[36] D. Bhattacharyya, N. Thirupathi Rao, E.S.N. Joshua, Y.-C. Hu, A bi-directional deep learning architecture for lung nodule semantic segmentation, The Visual Computer, 39(11) (2023) 5245-5261.